
NoiseGrad: enhancing explanations by introducing stochasticity to model weights

Kirill Bykov*

ML Group, TU Berlin, Germany
 UMI Lab
 TU Berlin
 kirill079@gmail.com

Anna Hedström*

ML Group, TU Berlin, Germany
 UMI Lab
 anna.hedstroem@tu-berlin.de

Shinichi Nakajima

ML Group, TU Berlin, Germany
 RIKEN AIP, Tokyo, Japan
 nakajima@tu-berlin.de

Marina M.-C. Höhne

ML Group, TU Berlin, Germany
 UMI Lab
 marina.hoehne@tu-berlin.de

Abstract

Attribution methods remain a practical instrument that is used in real-world applications to explain the decision-making process of complex learning machines. It has been shown that a simple method called SmoothGrad can effectively reduce the visual diffusion of gradient-based attribution methods and has established itself among both researchers and practitioners. What remains unexplored in research, however, is how explanations can be improved by introducing stochasticity to the model weights. In the light of this, we introduce — *NoiseGrad* — a stochastic, method-agnostic explanation-enhancing method that adds noise to the weights instead of the input data. We investigate our proposed method through various experiments including different datasets, explanation methods and network architectures and conclude that NoiseGrad (and its extension NoiseGrad++) with multiplicative Gaussian noise offers a clear advantage compared to SmoothGrad on several evaluation criteria. We connect our proposed method to Bayesian Learning and provide the user with a heuristic for choosing hyperparameters.

1 Introduction

The ubiquitous usage of Deep Neural Networks (DNNs), fueled by their ability to generalize and learn complex nonlinear functions, has presented both researchers and practitioners with the problem of non-interpretability and opaqueness of Machine Learning (ML) models. This lack of transparency, coupled with the widespread use of these highly complex models in practice, represents a risk and a major challenge for the responsible use of artificial intelligence, especially in security-critical areas, such as in the medical field. In response to this, the field of Explainable AI (XAI) has emerged with the aim of making the predictions of complex algorithms comprehensible for humans.

Thus far most of the progress was made at the *local* level of XAI i.e., explaining a model decision of an *individual* input [1] where various methods such as Layer-wise Relevance Propagation (LRP) [2], Deep Taylor Decomposition [3], CAM [4] and its extension GradCAM [5] and Integrated Gradient [6] have proven effective in explaining DNNs. Those gradient-based methods are popular because of their simplicity, however they tend to suffer from the gradient shattering effect, which often results in noisy explanation maps [7]. As a remedy, Smilkov et. al. proposed a simple solution called

*Both authors contributed equally to this work. Code and examples available at <https://github.com/understandable-machine-intelligence-lab/NoiseGrad>.

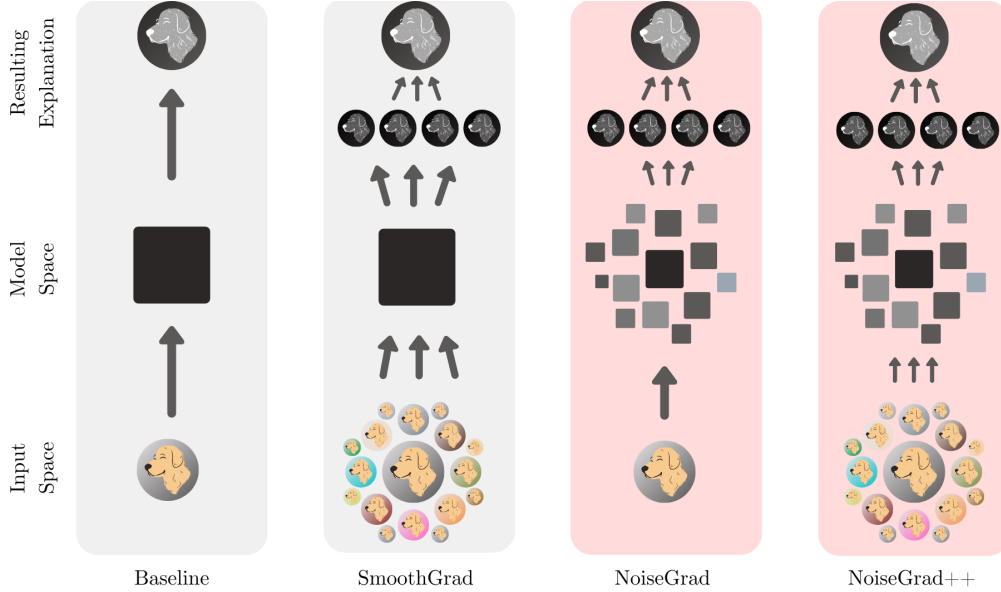


Figure 1: Illustration of our proposed methods: the functionality of the individual methods, i.e., Baseline, SmoothGrad, NoiseGrad and NoiseGrad++ are visualized schematically from left to right, each partitioned in input space, model space and the resulting explanation from bottom to top. The baseline explanations are computed in a deterministic fashion – one input (dog), one model (black square), one explanation. SmoothGrad enhances the explanation by exploring the neighborhood of a datapoint, here indicated by multiple noisy versions of the input. In contrast, our proposed method, NoiseGrad, enhances the explanations by investigating the neighborhood of the trained model, indicated by multiple versions of the model. NoiseGrad++ combines SmoothGrad and NoiseGrad by incorporating both stochasticities in the input space and model space.

SmoothGrad [8] where the local neighborhood of an input is taken into account for computing the explanation. In a nutshell, this is done by adding Gaussian noise to a given input n times, then calculating n explanations and finally averaging over all explanations results to one single explanation outcome. Hence SmoothGrad is applicable to any gradient-based explanation method and has been practically proven to reduce the visual noise of explanations.

The mechanism behind SmoothGrad’s enhancement of explanations is not yet well understood. One could argue that SmoothGrad averages out the shattering effect. However, SmoothGrad performs best when the added noise level is around 10%–20% of the signal level, which not only smooths out peaky derivatives but is large enough to cross the decision boundary. From this fact we derive the hypothesis that SmoothGrad perturbs the test sample in order to get a signal from the steepest part of the decision boundary. This motivated us to explore another way of using stochasticity: instead of adding noise to the input, our proposed method, called NoiseGrad (NG), draws samples from the network weights from a *tempered* Bayes posterior [9], such that the decision boundaries of some models are close to the test sample, which results in more precise explanations.

Our hypothesis leads to a natural and easy way of hyperparameter choice: the noise level (which corresponds to the temperature of the tempered Bayes posterior) is chosen such that the relative classification accuracy drop is around 5%. In addition, we empirically found that sampling from the tempered Bayes posterior can be approximated by multiplicative noise applied to the network weights – in the same spirit as MC dropout [10]. Thus, our proposed method NoiseGrad can be implemented as easily as SmoothGrad with an automatic hyperparameter choice and is applicable to any model architecture and explanation method. Our experiments empirically support our hypothesis and show quantitatively and qualitatively that NoiseGrad outperforms SmoothGrad and combining NoiseGrad with SmoothGrad, which we refer to as NoiseGrad++ (NG++), further boosts the performance. An overview of our proposed methods is given as an illustration in Figure 1.

The main contributions of this paper are summarized in the following

- We present a novel method **NoiseGrad** that improves attribution-based explanations by introducing stochasticity to the model parameters.
- In various experiments, we show qualitatively and quantitatively over different evaluation criteria that NoiseGrad performs favorably in comparison to SmoothGrad.
- We demonstrate that **NoiseGrad++**, a combination of both SmoothGrad and NoiseGrad, further boosts the quality of attributions.

2 Background

Let $f(\cdot; \hat{W}) : \mathbb{R}^d \rightarrow \mathbb{R}^k$ be a neural network with learned weights $\hat{W} \subset \mathbb{R}^S$, that maps a vector $\mathbf{x} \in \mathbb{R}^d$ from the input domain to a vector $y \in \mathbb{R}^k$ in the output domain. Attribution methods work as an operator $E(\mathbf{x}, f(\cdot, \hat{W}))$, that attributes relevances to the features of the input \mathbf{x} with respect to the model function $f(\cdot, \hat{W})$. More in-depth discussion about the different explainability methods can be found in the supplementary material.

2.1 Enhancing explanations by adding noise to the inputs

A recently proposed popular method — SmoothGrad — seeks to alleviate noise and visual diffusion of saliency maps by introducing stochasticity to the inputs [8]. SmoothGrad adds Gaussian noise to the input features of a given datapoint and the resulting explanation is obtained by averaging over explanations of the noisy versions of the input:

$$E_{SG}(\mathbf{x}) = \frac{1}{N} \sum_{i=1}^N E(\mathbf{x} + \xi_i, f(\cdot, \hat{W})), \quad \xi_i \sim \mathcal{N}(\mathbf{0}, \sigma_{SG}^2 \mathbf{I}),$$

where $\mathcal{N}(\mu, \Sigma)$ denotes the Normal distribution with mean μ and covariance Σ and \mathbf{I} is the identity matrix. In addition to improving explanations, SmoothGrad is reported to be more robust against adversarial attacks [11]. SmoothGrad averages the explanations of the neighborhood around an initial point \mathbf{x} , thus, providing an explanation, not for a particular input point, but rather interprets the decision-making process of the model for its local neighborhood.

2.2 Enhancing explanations by approximate Bayesian learning

From a statistical perspective, training DNNs with the most commonly used loss functions and regularizers, such as categorical cross-entropy for classification tasks or MSE for regression, can be seen as performing *maximum a-posteriori (MAP) learning*. Hence, resulting weights can be thought of as point estimates for the mode of the posterior distribution over the parameter space. Although MAP learning is efficient since networks learn only a fixed set of weights, any information about the curvature of the parameter space and the uncertainties of the weights is not considered.

Recent research showed that the incorporation of information about posterior distribution can enhance local explanations for DNNs [12]. Intuitively, in contrast to the MAP learning where point estimates of weights represent one deterministic decision-making strategy, a posterior distribution represents an infinite ensemble of models, which employ different strategies towards the prediction. By aggregating the variability of the decision-making processes of networks, we can obtain a broader outlook on the features that were used for the prediction, i.e., obtaining deeper insights into the models' behavior.

In Bayesian Learning, there exist a plethora of different methods for approximating the posterior distribution, such as Variational Inference [13, 14], MC dropout [10], Variational Dropout [15, 16], MCMC sampling [9], but most of them require a full retraining of the network. A handy method to a local approximation of the posterior distribution around a pretrained MAP is given by the *Laplace approximation* [17, 18], where the posterior is approximated by the second-order Taylor expansion around the mode \hat{W}

$$\log p(W \mid \mathcal{D}_{tr}) \approx \log p(\hat{W} \mid \mathcal{D}_{tr}) - \frac{1}{2}(W - \hat{W})^T H(W - \hat{W}).$$

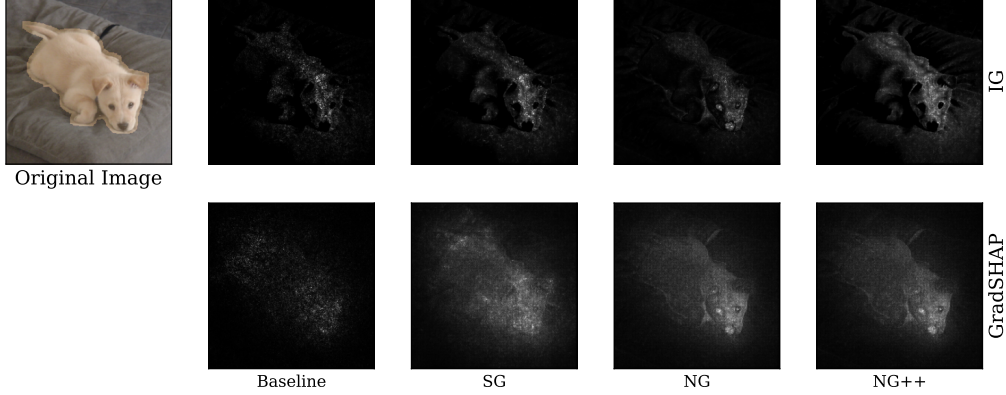


Figure 2: Illustration of the qualitative performance of Baseline, SG, NG and NG++ for two base explanation methods: Integrated Gradient (IG) [6] and GradientSHAP (GradSHAP) [20] for a randomly chosen image from the PASCAL VOC 2012 dataset with overlaid segmentation.

Here H is the Hessian of the negative log posterior at \hat{W} . This expression leads to a Gaussian approximation of the Bayes posterior

$$p(W \mid \mathcal{D}_{\text{tr}}) \approx N(W; \hat{W}, H^{-1}). \quad (1)$$

However, computing and inverting the full Hessian matrix is intractable for DNNs with more than thousands of weight parameters, and therefore different approximations methods were proposed, such as diagonal and tri-diagonal approximations. Recent developments in second-order optimization showed that Kronecker-factored Approximate Curvature (K-FAC) [19] can be used effectively to approximate the Hessian, even for complex DNNs with hundreds of thousands of parameters [18]. Such approximation of the Hessian does not require any retraining of the network, however, it requires the computation of the second-order statistics over the dataset, which can still be computationally expensive.

3 Method

As mentioned previously, the mechanism why SmoothGrad improves explanation has not been well understood. In empirical experiments we found that SmoothGrad with a suggested 10%–20% noise level is large enough to cross the decision boundary, resulting in a significant classification accuracy drop. Perhaps counter to intuition, this finding implies that SmoothGrad does not only smooth the peaky derivative but also collects signals from the steepest part of the likelihood, i.e., decision boundary, by perturbing the input sample with large noise.

Motivated by this observation, we propose another way of introducing stochasticity – instead of perturbing the input, we perturb the model itself. More precisely, we propose a new method — NoiseGrad — which draws samples from the network weights based on a *tempered* Bayes posterior [9], i.e., the Bayes posterior with the temperature higher than 1, such that the decision boundaries of some models are close to the test sample, to reinforce the signals for explanations. Mathematically, NG is expressed as follows

$$E_{\text{NG}}(\mathbf{x}) = \frac{1}{N} \sum_{i=1}^N E(\mathbf{x}, f(\cdot, \mathcal{W}_i)), \quad (2)$$

where $\{\mathcal{W}_i\}$ are samples drawn from a tempered Bayes posterior. Since approximate Bayesian learning is computationally expensive, we mainly focus on approximating the posterior with multiplicative Gaussian noise – in the spirit of MC dropout [10]: $\mathcal{W}_i = \hat{W} \cdot \eta_i$, where $\eta_i \sim \mathcal{N}(\mathbf{1}, \sigma_{\text{NG}}^2 \mathbf{I})$. Here, $\mathbf{1}$ is the vector with all entries equal to one. In this way, NoiseGrad can be viewed as a special case of Laplace approximation, where the posterior distribution is crudely approximated by

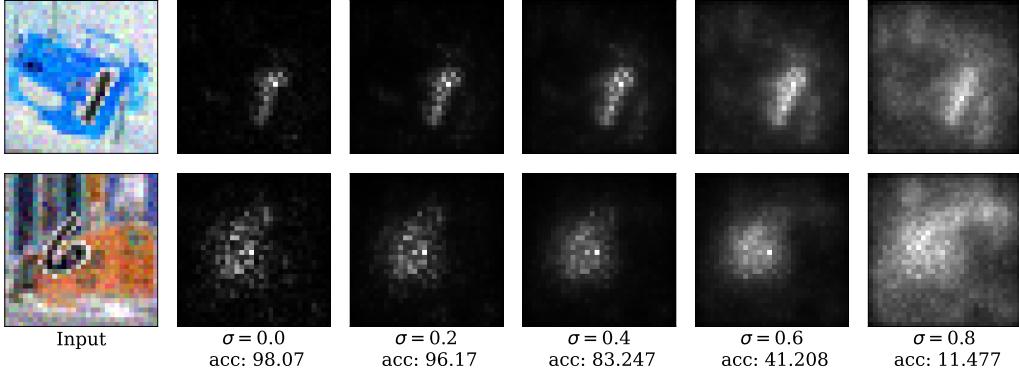


Figure 3: Illustration of NG-enhanced Saliency explanations on the CMNIST dataset: we observe an improvement of the localization ability of the explanation when increasing the hyperparameter σ until $\sigma \leq 0.4$ — afterwards, if the noise amplitude becomes too large, the models lose their predicting ability, which results in noisy attribution maps.

$N(W; \hat{W}, \sigma_{\text{NG}} \hat{W})$. By averaging over a sufficiently large number of samples N , we expect NG to smooth the signal and also collect amplified signals from models whose decision boundary is close to the test sample. Furthermore, to incorporate both stochasticities in the input space and the model space, we propose NoiseGrad++ as a combination of both NoiseGrad and SmoothGrad

$$E_{\text{NG++}}(\mathbf{x}) = \frac{1}{N} \sum_{i=1}^N \frac{1}{M} \sum_{j=1}^M E(\mathbf{x} + \xi_j, f(\cdot, \mathcal{W}_i)), \quad (3)$$

where $\xi_j \sim \mathcal{N}(\mathbf{0}, \sigma_{\text{SG}}^2 \mathbf{I})$ and N and M denote the number of models and noisy versions of input, respectively. In our experiments, NG++ further boosts the performance of NG, providing the best qualitative and quantitative performance.

Noise level. The important question is how much noise σ_{NG} should be added to the weights. Do we need to adjust the noise level, depending on the given model architecture or the dataset? We put forward a simple hypothesis: since we need signals from the models whose decision boundary is close to the test samples, we might choose the noise level σ_{NG} such that we observe a certain accuracy drop. From experimental results (discussed more in-depth in the supplementary material) we recommend to set the relative accuracy drop $\text{AD}(\sigma) = 1 - (\text{ACC}(\sigma) - \text{ACC}(\infty)) / (\text{ACC}(0) - \text{ACC}(\infty))$ to around 5% where $\text{ACC}(\sigma)$ denotes the classification accuracy at the noise level σ . Note that $\text{ACC}(0)$ and $\text{ACC}(\infty)$ correspond to the original accuracy and the chance level, respectively. This rule of thumb can be used for various model architectures with different scales, as discussed in Section 5.2.

4 Experiments

To evaluate our proposed methods, we are interested in comparing the *attribution quality* of NoiseGrad and NoiseGrad++ explanations with those produced by SmoothGrad. For this purpose, we now describe the specifics concerning the empirical experiments including datasets, evaluation methodology, comparison methods and models.

4.1 Datasets

To measure the goodness of an explanation, one typically needs to resort to proxies for evaluation since no ground-truth for explanations exists. Similar to [21] and [22] we therefore design a controlled setting for which the ground-truth segmentation labels are available. For this purpose, we construct a semi-natural dataset CMNIST (customized-MNIST), where each MNIST digit [23] is displayed on a randomly selected CIFAR background [24]. To ensure that the explainable evidence for a class lies in the vicinity of the object itself, rather than in its contextual surrounding, we uniformly

distribute CIFAR backgrounds for each MNIST digit class as we construct the CMNIST dataset. ground-truth segmentation labels for the explanations are formed by creating different variations of segmentation masks around the object of interest such as a squared box around the object or the pixels of the object itself. Moreover, we use the PASCAL VOC 2012 object recognition dataset [25] for evaluation, where the object localization masks are available. Further details on training- and test splits, preprocessing steps and other relevant dataset statistics can be found in the supplementary material. Naturally, the question arises whether object localization masks can be used as ground-truth labels for explanations of natural datasets in which the independence of the models from the background cannot be guaranteed. We therefore report quantitative metrics only on the controlled semi-natural dataset but report qualitative results on the natural dataset as well.

4.2 Evaluation methodology

While the debate of what properties an attribution-based explanation ought to fulfill continues, several works [3, 26, 27] suggest that in order to produce human-meaningful explanations one metric alone is not enough. To broaden the view of what it means to provide a good explanation, we evaluate the explanation-enhancing methods using three well-studied properties. Having the object segmentation masks available for the input images, we can formulate the first property as follows

(Property 1) Localization *measures the extent to which an explanation attributes its explainable evidence to the object of interest.*

The higher the concentration of attribution mass on the ground-truth mask the better. For this purpose, there exist many metrics in the literature [21, 28, 29, 30, 31, 32] that can be applied. Since we are interested in the attributions' rankings, we apply the Area Under the Receiver Operating Characteristic Curve (AUC) [32] (using Trapezoid rule) as a single metric in order to assess the explanation localization.

(Property 2) Faithfulness *estimates how the presence (or absence) of features influence the prediction score: removing highly important features results in model performance degradation.*

The second property attempts to understand whether the assigned attributions accurately reflect the behavior of the model. It is arguably one of the most well-studied evaluation metrics, hence many empirical interpretations have been proposed [2, 3, 33, 34]. To evaluate the relative fulfillment of this property, we conduct an experiment that iteratively modifies an image to measure the rank correlation between the sum of attributions for each modified patch and the difference in the prediction score [35]. Given a model f , an explanation function E and a subset $|S|$ of d indices of samples \mathbf{x} and a baseline value \bar{x} , we define faithfulness as follows

$$\mu_F(f, E; \mathbf{x}) = \text{corr}_{S \in \binom{[d]}{|S|}} \left(\sum_{i \in S} E(f, \mathbf{x})_i, f(\mathbf{x}) - f(\mathbf{x}_{[x_s = \bar{x}_s]}) \right) \quad (4)$$

Due to the potential appearance of spurious correlations and creation of out-of-distribution samples, while masking original input [36], the choice of the pixel perturbation strategy is non-trivial [6, 37]. For each method, we therefore enumerate over different combinations of patch-sizes and baseline values as we repeat the experiment for several test images. Further details on the perturbation strategies can be found in the Supplement.

(Property 3) Robustness *measures how strongly the explanations vary within a small local neighborhood of the input point while the model prediction remains approximately the same.*

In the third property to assess attribution quality, we examine the reliability of the explanation function [38, 39] which, with subtle variations also is referred to as *continuity* [3], *stability* [39], *coherence* [40] and *sensitivity* [34]. Similar to [11], we test the property by constructing a perturbed version of the input $\mathbf{x}' = \mathbf{x} + \delta$ by adding Gaussian noise such that $\delta \sim \mathcal{N}(0, \sigma^2)$. With some similarity function $S(\cdot)$ we measure the extent to which explanations of \mathbf{x} and \mathbf{x}' remained the same under the perturbation $E(\mathbf{x}) \approx E(\mathbf{x}')$ such that $S(E(\mathbf{x}), E(\mathbf{x}')) \approx 1$. Following up on the works of [41], we employ Kendall's tau rank correlation metric [42] for both Property 2 and 3 in the experiments.

4.3 Comparing methods and models

NoiseGrad is *method-agnostic* which means that it can be applied in conjunction with any explanation method. However, due to space limitations, we focus on post-hoc gradient-based explanation methods and use *Saliency* (SA) [43] as the base explanation method in the experiments. Since the majority of model-aware local explanation methods make use of the model gradients, we argue that a potential explanation improvement on SA with our proposed method may also be transferred to an improvement of a related gradient-based explanation method. As the comparative baseline explanation method (Baseline), we use the Saliency explanation, which adds no noise to either the weights or the inputs.

Explanations were produced for networks of different architectural composition, such as ResNet [44], VGG [45] and LeNet [46]. All networks were trained for image classification tasks so that they showcased a comparable test accuracy to a minimum of 86% and 92% classification accuracy for CMNIST and PASCAL VOC 2012 datasets respectively. For more details on the model architectures, optimization configurations and training results, we refer to the supplementary material.

5 Results

In the following, we present our experimental results. The findings can be summarized as follows: (i) both NG and NG++ offer an advantage over SG measured with several metrics of attribution quality and (ii) as a heuristic, choosing the hyperparameters for NG and NG++ according to a classification performance drop of 5% typically results in explanations with a high attribution quality.

5.1 Benchmarking methods

We start by examining the performance of the methods considering the three aforementioned attribution quality criteria applied to the absolute values of their respective explanations. The results are summarized in Table 1, where the methods (Baseline, SG, NG, NG++) are stated in the first column and the respective values for localization, faithfulness and robustness in column 2-4. The scores were computed as average over 200 randomly chosen test images from CMNIST using a ResNet9 classification model and the Saliency method for computing the explanations. Note that the calculation of the faithfulness scores is computationally expensive since we recompute for different patch sizes and baseline values, we only use 50 random samples out of the 200 test samples. In order to obtain the optimal value for the hyperparameters of NG and NG++, we perform a grid search over σ values for each method SG, NG and NG++ separately, such that it maximized the localization quality, i.e., the AUC value.

From Table 1, we can observe a significant attribution quality boost by SG, NG and NG++ in comparison to the Baseline method, where no noise is added. For each of the examined quality criteria, the values range between $[0, 1]$, where higher values are better, the combination of SmoothGrad and NoiseGrad, i.e., NG++ is significantly better than either method alone. Furthermore, we can observe that NG outperforms SG in terms of localization and robustness but not in terms of faithfulness.

Table 1: Comparison of Attribution Quality

Method	Localization AUC	Faithfulness $\mu_F(f, E; \mathbf{x})$	Robustness $S(E(\mathbf{x}), E(\mathbf{x}'))$
Baseline	0.9278 \pm 0.0250	0.2274 \pm 0.1599	0.4037 \pm 0.0627
SG	0.9783 \pm 0.0131	0.2690 \pm 0.1579	0.5072 \pm 0.1167
NG	0.9795 \pm 0.0120	0.2457 \pm 0.1587	0.5492 \pm 0.0733
NG++	0.9830 \pm 0.0111	0.2796 \pm 0.1454	0.5701 \pm 0.0980

Hyperparameter search for NG++. The optimal hyperparameters for NG++ were estimated by a grid search shown in Figure 4 (left). For all experiments relevant to NG++ we set $N=10$ and let the stepsize equal to 0.1 and 0.2 for σ_{NG} (x-axis) and σ_{SG} (y-axis) respectively. To more clearly observe how adding noise to the weights (or inputs) changes the attribution quality in relation to the baseline, we compare the *relative AUC improvement* from baseline, i.e., $dAUC$, which is calculated as follows: $(AUC / AUC_{Baseline}) - 1$. Dark red indicates better attribution quality compared to the baseline and dark blue suggests deterioration in the explanation localization.

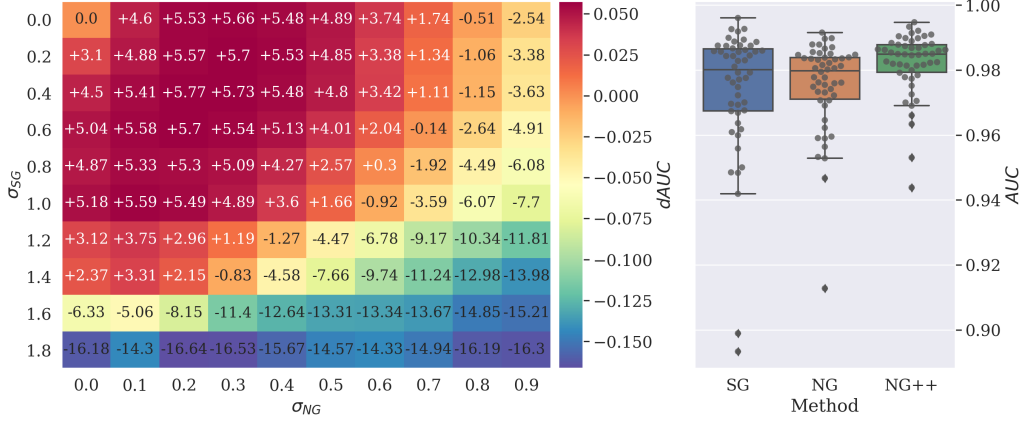


Figure 4: Left: visualization of the grid search results for the hyperparameter search for NG++, measured with $dAUC$, where the x-axis show σ_{NG} and the y-axis show σ_{SG} . Right: visualization of the AUC results when using the optimal hyperparameters for all three methods: SG, NG and NG++. We observe that NG++ surpasses both SG and NG with respect to localisation.

Most interestingly, optimal results can be obtained when combining NG and SG to NG++ with $\sigma_{SG}=0.4$ and $\sigma_{NG}=0.2$. From Figure 4, we can moreover observe that for values higher than $\sigma_{NG} \leq 0.7$ or $\sigma_{SG} \leq 1.4$ respectively, adding noise improves attribution quality. Interestingly, we find that explanations with SG make $dAUC$ deteriorate over 10 times faster than explanations using NG. When comparing the first column (SG, only input noise is applied) and the first row (NG, only noise to model weights is applied) we can draw the conclusion that attribution quality is, in general, higher for NoiseGrad than for SmoothGrad. Lastly, to attain a more nuanced view of the results, we study the distribution of $dAUC$ scores for the different approaches as depicted in Figure 4 (right). Notable is that scores of NG and SG are comparable, whilst for NG++ the attribution quality of explanations is significantly higher.

5.2 Heuristic for the hyperparameter choice

NoiseGrad and NoiseGrad++ come with two hyperparameters σ and N that require tuning. As observed by the dark blue colours in Figure 4, not every combination of σ_{NG} and σ_{SG} will increase the attribution quality. On the contrary, some values of σ for NG++ can make attribution quality deteriorate. As such, we dedicate the following paragraphs to describe how to best choose these hyperparameters.

Choosing σ_{NG} . In developing a heuristic for σ_{NG} , we set up an experiment where we record AUC scores and drop in model accuracy for different network architectures – as we increased the level of noise. From this analysis (as further discussed in the supplementary material), we could conclude that the optimal noise level for σ_{NG} is where the classification accuracy drops by $\sim 5\%$ (since this is where AUC curves typically peaks).

Table 2: Resulting AUC scores for different architectures, with applied heuristic

Method	LeNet	VGG11	ResNet9	ResNet18	ResNet50
Base	0.923 ± 0.033	0.962 ± 0.015	0.930 ± 0.024	0.911 ± 0.037	0.909 ± 0.034
SG	0.950 ± 0.029	0.980 ± 0.011	0.969 ± 0.017	0.951 ± 0.030	0.941 ± 0.032
NG	0.950 ± 0.028	0.982 ± 0.010	0.977 ± 0.012	0.966 ± 0.022	0.967 ± 0.021
NG++	0.955 ± 0.023	0.985 ± 0.006	0.974 ± 0.012	0.961 ± 0.026	0.954 ± 0.029

To verify that the heuristic indeed increase the attribution quality, we next apply the rule of thumb for NG and NG++ explanations and record the AUC values. For computing the SG explanations, we followed the authors’ suggestion [8] for choosing the optimal σ -level. As observed from the

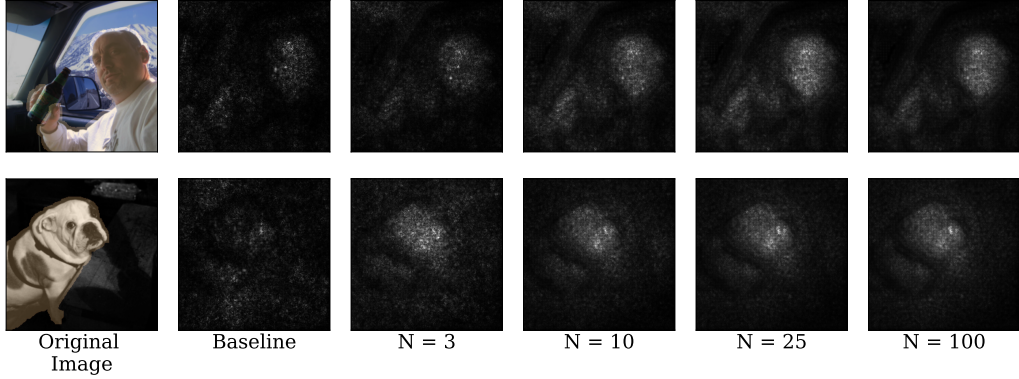


Figure 5: Saliency explanations for two randomly chosen PASCAL VOC 2012 images using NoiseGrad with different sample sizes. The quality of the explanation improves with an increasing number of samples until it no longer changes when the number of samples reaches 25.

Table 2, regardless of architectural set-up, adding noise to the weights (either through NG or NG++) significantly offers an advantage compared to SG and baseline.

Choosing N . Proposed NG and NG++ methods can be seen as a version of a Monte-Carlo integration [47] for the following integrals:

$$I_{NG}(\mathbf{x}) = \int_{\mathbb{R}^S} E(\mathbf{x}, f(\cdot, \mathcal{W})) p(\mathcal{W}) d\mathcal{W},$$

$$I_{NG++}(\mathbf{x}) = \int_{\mathbb{R}^S} \int_{\mathbb{R}^d} E(\mathbf{x} + \xi, f(\cdot, \mathcal{W}_i)) p(\xi) p(\mathcal{W}) d\xi d\mathcal{W}.$$

As a Monte-Carlo approximation, the standard error of the mean decreases asymptotically as $\frac{1}{\sqrt{N}}$ is independent from the dimensionality of the integral. In practice, we observe that a sample size $N \in [25, 50]$ is already sufficient to generate appealing explanations as shown in Figure 5. For NG++, only 10 samples for both N (NG samples) and M (SG samples) are enough to enhance explanations.

6 Discussion and Conclusion

In this paper, we present a novel method called *NoiseGrad* which is a simple, method-agnostic explanation-enhancing approach that explores how introducing stochasticity to the model parameters can increase attribution quality. We evidence on a diverse set of evaluation criteria that NoiseGrad and especially its extension NoiseGrad++ can outperform SmoothGrad while using a simple heuristic for the choice of hyperparameters.

Limitations. The main limitation of NG and NG++ is that their performance depends on the choice of the noise level, where more noise is not always better. In response to this, we put forward a heuristic based on model accuracy that makes it easy for the user to set an appropriate noise level. Furthermore, since the number of parameters in a DNN is usually larger than the number of features in the data, NoiseGrad becomes slightly more computationally extensive than SmoothGrad. In addition, explanation evaluation is still an unsolved problem in XAI research and it is without doubt that each evaluation technique comes with individual drawbacks. To this end, we therefore apply several quality criteria, that is, localization, faithfulness and robustness to assess our methods quantitatively.

Future work. To broaden the applicability of our proposed methods, we are interested in quantitatively validating to what extent localization as an attribution quality criteria is useful on natural datasets. In addition, it would be interesting to further investigate the performance of NG and NG++ on other tasks than image classification such as time-series prediction or NLP. We also want to explore alternative ways of adding noise to weights of a neural network, e.g., by adding different levels of noise to different layers or individual neurons.

References

- [1] Riccardo Guidotti et al. “A survey of methods for explaining black box models”. In: *ACM computing surveys (CSUR)* 51.5 (2018), pp. 1–42.
- [2] Sebastian Bach et al. “On pixel-wise explanations for non-linear classifier decisions by layer-wise relevance propagation”. In: *PloS one* 10.7 (2015).
- [3] Grégoire Montavon, Wojciech Samek, and Klaus-Robert Müller. “Methods for interpreting and understanding deep neural networks”. In: *Digital Signal Processing* 73 (2018), pp. 1–15.
- [4] Bolei Zhou et al. “Learning deep features for discriminative localization”. In: *Proceedings of the IEEE conference on computer vision and pattern recognition*. 2016, pp. 2921–2929.
- [5] Ramprasaath R. Selvaraju et al. “Grad-CAM: Visual Explanations from Deep Networks via Gradient-Based Localization”. In: *International Journal of Computer Vision* 128.2 (Oct. 2019), pp. 336–359. ISSN: 1573-1405. DOI: 10.1007/s11263-019-01228-7. URL: <http://dx.doi.org/10.1007/s11263-019-01228-7>.
- [6] Mukund Sundararajan, Ankur Taly, and Qiqi Yan. “Axiomatic attribution for deep networks”. In: *International Conference on Machine Learning*. PMLR. 2017, pp. 3319–3328.
- [7] Wojciech Samek et al. “Explaining deep neural networks and beyond: A review of methods and applications”. In: *Proceedings of the IEEE* 109.3 (2021), pp. 247–278.
- [8] Daniel Smilkov et al. “Smoothgrad: removing noise by adding noise”. In: *arXiv preprint arXiv:1706.03825* (2017).
- [9] F. Wenzel et al. “How Good is the Bayes Posterior in Deep Neural Networks Really?” In: *arXiv:2002.02405* (2020).
- [10] Y. Gal and Z. Ghahramani. “Dropout as a Bayesian Approximation: Representing Model Uncertainty in Deep Learning”. In: *Proceedings of ICML*. 2016.
- [11] Ann-Kathrin Dombrowski et al. “Explanations can be manipulated and geometry is to blame”. In: *Advances in Neural Information Processing Systems*. 2019, pp. 13567–13578.
- [12] Kirill Bykov et al. “How Much Can I Trust You?—Quantifying Uncertainties in Explaining Neural Networks”. In: *arXiv preprint arXiv:2006.09000* (2020).
- [13] A. Graves. “Practical variational inference for neural networks”. In: *Advances in NIPS*. 2011.
- [14] K. Osawa et al. “Practical Deep Learning with Bayesian Principles”. In: *Advances in NeurIPS*. 2019.
- [15] D. P. Kingma, T. Salimans, and M. Welling. “Variational Dropout and the Local Reparameterization Trick”. In: *Advances in NIPS*. 2015.
- [16] D. Molchanov, A. Ashukha, and D. Vetrov. “Variational Dropout Sparsifies Deep Neural Networks”. In: *Proceedings of ICML*. 2017.
- [17] David JC MacKay. “A practical Bayesian framework for backpropagation networks”. In: *Neural computation* 4.3 (1992), pp. 448–472.
- [18] Hippolyt Ritter, Aleksandar Botev, and David Barber. “A scalable laplace approximation for neural networks”. In: *6th International Conference on Learning Representations, ICLR 2018-Conference Track Proceedings*. Vol. 6. International Conference on Representation Learning. 2018.
- [19] James Martens and Roger Grosse. “Optimizing neural networks with kronecker-factored approximate curvature”. In: *International conference on machine learning*. 2015, pp. 2408–2417.
- [20] Scott M Lundberg and Su-In Lee. “A unified approach to interpreting model predictions”. In: *Advances in neural information processing systems*. 2017, pp. 4765–4774.
- [21] Leila Arras, Ahmed Osman, and Wojciech Samek. *Ground Truth Evaluation of Neural Network Explanations with CLEVR-XAI*. 2021. arXiv: 2003.07258 [cs.CV].
- [22] Mengjiao Yang and Been Kim. “Benchmarking Attribution Methods with Relative Feature Importance”. In: *CoRR* abs/1907.09701 (2019).
- [23] Yann LeCun, Corinna Cortes, and CJ Burges. “MNIST handwritten digit database”. In: *ATT Labs [Online]*. Available: <http://yann.lecun.com/exdb/mnist> 2 (2010).
- [24] Alex Krizhevsky. *Learning multiple layers of features from tiny images*. Tech. rep. 2009.
- [25] M. Everingham et al. “The Pascal Visual Object Classes (VOC) Challenge”. In: *International Journal of Computer Vision* 88.2 (June 2010), pp. 303–338.
- [26] David Alvarez-Melis and Tommi S Jaakkola. “Towards robust interpretability with self-explaining neural networks”. In: *arXiv preprint arXiv:1806.07538* (2018).
- [27] Diogo V Carvalho, Eduardo M Pereira, and Jaime S Cardoso. “Machine learning interpretability: A survey on methods and metrics”. In: *Electronics* 8.8 (2019), p. 832.
- [28] Jonas Theiner, Eric Müller-Budack, and Ralph Ewerth. *Interpretable Semantic Photo Geolocalization*. 2021. arXiv: 2104.14995 [cs.CV].
- [29] Sebastian Bach et al. *Analyzing Classifiers: Fisher Vectors and Deep Neural Networks*. 2015. arXiv: 1512.00172 [cs.CV].

- [30] Maximilian Kohlbrenner et al. *Towards Best Practice in Explaining Neural Network Decisions with LRP*. 2020. arXiv: 1910.09840 [cs.LG].
- [31] Jianming Zhang et al. *Top-down Neural Attention by Excitation Backprop*. 2016. arXiv: 1608.00507 [cs.CV].
- [32] Tom Fawcett. “An Introduction to ROC Analysis”. In: *Pattern Recogn. Lett.* 27.8 (June 2006), pp. 861–874. ISSN: 0167-8655. DOI: 10.1016/j.patrec.2005.10.010. URL: <https://doi.org/10.1016/j.patrec.2005.10.010>.
- [33] Wojciech Samek et al. “Evaluating the visualization of what a deep neural network has learned”. In: *IEEE transactions on neural networks and learning systems* 28.11 (2016), pp. 2660–2673.
- [34] Chih-Kuan Yeh et al. “On the (in) fidelity and sensitivity for explanations”. In: *arXiv preprint arXiv:1901.09392* (2019).
- [35] Umang Bhatt, Adrian Weller, and José M. F. Moura. *Evaluating and Aggregating Feature-based Model Explanations*. 2020. arXiv: 2005.00631 [cs.LG].
- [36] Sara Hooker et al. *A Benchmark for Interpretability Methods in Deep Neural Networks*. 2019. arXiv: 1806.10758 [cs.LG].
- [37] Pascal Sturmfels, Scott Lundberg, and Su-In Lee. “Visualizing the Impact of Feature Attribution Baselines”. In: *Distill* (2020). <https://distill.pub/2020/attribution-baselines>. DOI: 10.23915/distill.00022.
- [38] Pieter-Jan Kindermans et al. “The (un) reliability of saliency methods”. In: *Explainable AI: Interpreting, Explaining and Visualizing Deep Learning*. Springer, 2019, pp. 267–280.
- [39] David Alvarez-Melis and Tommi S. Jaakkola. *Towards Robust Interpretability with Self-Explaining Neural Networks*. 2018. arXiv: 1806.07538 [cs.LG].
- [40] Riccardo Guidotti et al. *Black Box Explanation by Learning Image Exemplars in the Latent Feature Space*. 2020. arXiv: 2002.03746 [cs.CV].
- [41] Jiefeng Chen et al. “Robust attribution regularization”. In: *Advances in Neural Information Processing Systems*. 2019, pp. 14300–14310.
- [42] Maurice G Kendall. “A new measure of rank correlation”. In: *Biometrika* 30.1/2 (1938), pp. 81–93.
- [43] Avanti Shrikumar, Peyton Greenside, and Anshul Kundaje. “Learning important features through propagating activation differences”. In: *International Conference on Machine Learning*. PMLR, 2017, pp. 3145–3153.
- [44] Kaiming He et al. *Deep Residual Learning for Image Recognition*. 2015. arXiv: 1512.03385 [cs.CV].
- [45] Karen Simonyan and Andrew Zisserman. “Very deep convolutional networks for large-scale image recognition”. In: *arXiv preprint arXiv:1409.1556* (2014).
- [46] Yann LeCun et al. “Gradient-based learning applied to document recognition”. In: *Proceedings of the IEEE* 86.11 (1998), pp. 2278–2324.
- [47] Nicholas Metropolis and Stanislaw Ulam. “The monte carlo method”. In: *Journal of the American statistical association* 44.247 (1949), pp. 335–341.
- [48] Radford M Neal. “Bayesian learning via stochastic dynamics”. In: *Advances in neural information processing systems*. 1993, pp. 475–482.
- [49] Adam D Cobb and Brian Jalaian. “Scaling Hamiltonian Monte Carlo Inference for Bayesian Neural Networks with Symmetric Splitting”. In: *arXiv preprint arXiv:2010.06772* (2020).
- [50] Jongseok Lee et al. “Estimating Model Uncertainty of Neural Networks in Sparse Information Form”. In: *International Conference on Machine Learning (ICML)*. Proceedings of Machine Learning Research. 2020.
- [51] Guozhong An. “The effects of adding noise during backpropagation training on a generalization performance”. In: *Neural computation* 8.3 (1996), pp. 643–674.
- [52] Ben Poole, Jascha Sohl-Dickstein, and Surya Ganguli. “Analyzing noise in autoencoders and deep networks”. In: *arXiv preprint arXiv:1406.1831* (2014).
- [53] Charles Blundell et al. “Weight uncertainty in neural network”. In: *International Conference on Machine Learning*. PMLR, 2015, pp. 1613–1622.
- [54] Thomas G Dietterich. “Ensemble methods in machine learning”. In: *International workshop on multiple classifier systems*. Springer, 2000, pp. 1–15.
- [55] Laura Rieger and Lars Kai Hansen. “A simple defense against adversarial attacks on heatmap explanations”. In: *arXiv preprint arXiv:2007.06381* (2020).
- [56] Adam Paszke et al. “PyTorch: An Imperative Style, High-Performance Deep Learning Library”. In: *Advances in Neural Information Processing Systems* 32. Ed. by H. Wallach et al. Curran Associates, Inc., 2019, pp. 8024–8035. URL: <http://papers.neurips.cc/paper/9015-pytorch-an-imperative-style-high-performance-deep-learning-library.pdf>.
- [57] M. Everingham et al. *The PASCAL Visual Object Classes Challenge 2012 (VOC2012) Results*. <http://www.pascal-network.org/challenges/VOC/voc2012/workshop/index.html>.

- [58] Christopher J Anders et al. "Understanding patch-based learning of video data by explaining predictions". In: *Explainable AI: Interpreting, Explaining and Visualizing Deep Learning*. Springer, 2019, pp. 297–309.
- [59] Leila Arras et al. "' What is relevant in a text document?': An interpretable machine learning approach". In: *PloS one* 12.8 (2017), e0181142.
- [60] Grégoire Montavon et al. "Layer-wise relevance propagation: an overview". In: *Explainable AI: Interpreting, Explaining and Visualizing Deep Learning*. Springer, 2019, pp. 193–209.
- [61] Ilya Loshchilov and Frank Hutter. *Decoupled Weight Decay Regularization*. 2019. arXiv: 1711.05101 [cs.LG].
- [62] Jia Deng et al. "Imagenet: A large-scale hierarchical image database". In: *2009 IEEE conference on computer vision and pattern recognition*. Ieee. 2009, pp. 248–255.

Supplementary material

A Heuristic for choosing hyperparameters

For each explanation-enhancing method, we clarify the recommended heuristic i.e., the rule of thumb that was applied in the experiments to choose the right level of noise.

SmoothGrad. As suggested by the authors in [8], we set the standard deviation of the input noise as follows

$$\sigma_{\text{SG}} = \alpha_{\text{SG}}(\max(x) - \min(x)), \quad (5)$$

where x is the input image and α_{SG} the noise level, which is recommended by the authors to be in the interval $[0.1, 0.2]$. We set $\alpha_{\text{SG}} = 0.2$ since with this noise level, SmoothGrad produced the explanations with the highest attribution quality in most of the cases in our experiments.

NoiseGrad. We choose σ_{NG} such that the relative accuracy drop $\text{AD}(\sigma_{\text{NG}})$ is approximately 5 percent in all experiments. We defined the relative accuracy drop as follows:

$$\text{AD}(\sigma) = 1 - \frac{\text{ACC}(\sigma) - \text{ACC}(\infty)}{\text{ACC}(0) - \text{ACC}(\infty)} \quad (6)$$

, where $\text{ACC}(0)$ and $\text{ACC}(\infty)$ correspond to the original accuracy and the chance level, respectively.

NoiseGrad++. We fix the noise level σ_{SG} for SG by Eq. (5) (setting the noise level to $\alpha_{\text{SG}} = 0.1$ i.e., the lower bound of the noise interval as suggested in [8]) and adjust the noise level σ_{NG} for NG so that the relative accuracy drop

$$\text{AD}_{++}(\sigma_{\text{SG}}, \sigma_{\text{NG}}) = 1 - \frac{\text{ACC}_{++}(\sigma_{\text{SG}}, \sigma_{\text{NG}}) - \text{ACC}(\infty)}{\text{ACC}_{++}(0, 0) - \text{ACC}(\infty)} \quad (7)$$

is again around $\alpha_{\text{NG++}} = 0.05$. Here, $\text{ACC}_{++}(\sigma_{\text{SG}}, \sigma_{\text{NG}})$ is the classification accuracy with noise levels σ_{SG} and σ_{NG} in the input image and the weight parameters, respectively.

For a better comprehension of the recommended heuristic, we report the relation between AUC value, i.e., the localization quality of the explanations and the accuracy drop of the model (ACC) (see Eq. 6) in Figure 6. The more noise added to the weights, the higher is the accuracy drop, which is reported on the x-axis. Interestingly, we observe an increase in the AUC value, reported on the y-axis, until an accuracy drop of 5 percent. Adding more noise to the weights leads to a greater accuracy drop and causes the AUC values to decrease again.

B Connection to Diagonal and KFAC Laplace approximation

As described in the main manuscript, NoiseGrad with multiplicative Gaussian noise can be seen as performing a quite crude Laplace Approximation. Yet, despite the simplicity of the proposed method, it is still sufficiently accurate to get an insight into the uncertainty of the model in order to enhance explanations.

We illustrate uncertainties obtained by our proposed method on a toy-task – a one-dimensional regression generated by a Gaussian Process with RBF kernel with parameters $l = 1$, $\sigma = 0.3$. In total we generated 400 points, 250 were used for training and 150 for testing. For training, we used a simple two-layer MLP with 10 hidden neurons respectively and sampled 1000 models using Hamiltonian Monte Carlo [48] using the `hamiltonch` library [49]. The sampled model used to perform both Kroneker-Factored (KF) and Diagonal Laplace Approximations using the `curvature` library [50]. Finally, we visualise the uncertainty of the predictions by adding multiplicative noise to the weights using NoiseGrad, comparing it to the KFAC and Diagonal Laplace approximations. Hyperparameters for all three methods were chosen in order to have approximately the same loss on the test set. All results are shown in Figure 7, which demonstrates that NoiseGrad has not quite as precise, but a similar estimate of the model uncertainty as the Bayesian approximation methods.

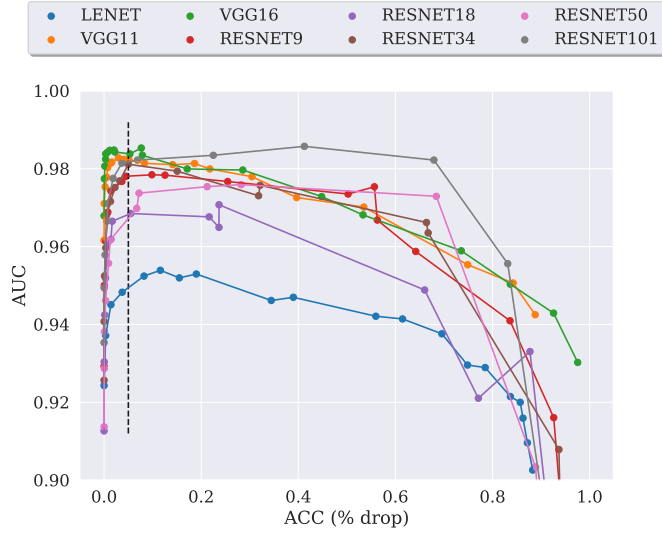


Figure 6: A visual interpretation of the proposed "5 percent accuracy drop" noise heuristic. Each line represents a different model architecture used in the CMNIST experiment and every dot reflects the average results from 200 randomly test samples. We can observe in that general, an increase in the noise level until a drop in accuracy of $\alpha_{\text{NG}} = 0.05$ (black horizontal line), boosts attribution quality (AUC value).

Empirically, from Figure 8, we can observe that explanations, which were enhanced by NoiseGrad have only slight visual differences compared to the explanations obtained by proper Laplace Approximation methods, i.e., Diagonal or KFAC. For this experiment we performed Laplace Approximation on ResNet18, trained for multi-label classification on the PASCAL VOC 2012 dataset. Setting the NoiseGrad hyperparameter σ to 0.1 we searched for the hyperparameters of Diagonal and KFAC Laplace approximation such that the all models had in average a similar performance on the test data.

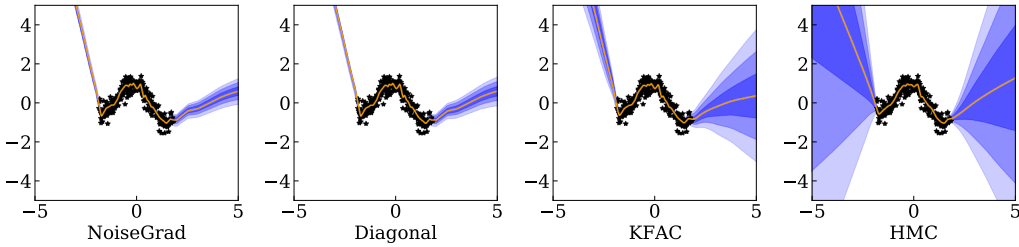


Figure 7: Toy example: comparison of NoiseGrad with Diagonal, KFAC and Hamiltonian Monte Carlo Approximation. Parameters for the NoiseGrad, Diagonal and KFAC Laplace approximations were chosen, such that they have a similar performance (MSE loss) on thee test dataset.

C Related Works

While adding an element of stochasticity during back-propagation to improve generalization performance is nothing new in the Machine Learning community [51, 10, 52, 53] – to the best of our knowledge, this is the first time when the intent is to improve explanations.

Most similar to our proposed NoiseGrad method are approaches that also inject stochasticity at inference time e.g., [10] which we also do. Our method can further be associated with *ensemble modelling* [54], where an ensemble of predictions from several classifiers are averaged, in order to increase the representation of the model space or simply, reduce the risk of choosing a sub-optimal

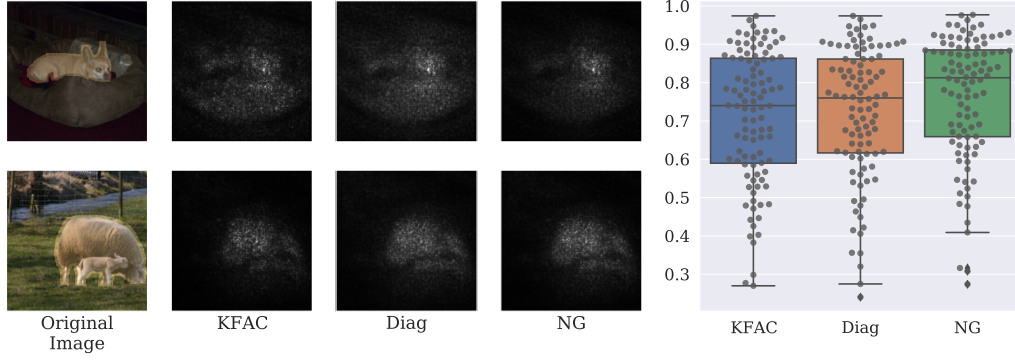


Figure 8: Comparison of the performance between our proposed method NG, KFAC and Diagonal Laplace Approximation. We can observe that the attribution quality (left: for 2 randomly chosen images) is comparable both visually and quantitatively (right: measured by AUC) for the different approximation methods.

classifier. Ensemble modelling is motivated by the idea of "*wisdom of the crowd*", where a decision is based on the collective opinion of several experts (models) rather than relying on a single expert opinion (single model). In our proposed method, by averaging over a sufficiently large number of samples N , the idea is that the noise associated with each individual explanation will be approximately eliminated.

SmoothGrad [8] – being the main comparative method of this work – has gained a great amount of popularity since its publication. That being said, to our awareness, very few additions have been put forward when it comes to extending the idea of averaging explanations from noisy input samples. However, in the simple operation of *averaging* in order to enhance explanations, a few ideas have been proposed. The work by [35] shows that the typical error of aggregating explanation functions is less than the expected error of an explanation function alone and [55] suggests a simple technique of averaging multiple explanation methods to improve robustness against manipulation.

D Experiments

In the following, we will provide additional information regarding the experimental setup as described in the main manuscript. All experiments were computed on Tesla P100-PCIE-16GB GPUs.

D.1 Evaluation parameters

In the main manuscript, we presented three *desirable* properties that we deemed useful for an explanation to fulfill. To measure the extent to which the explanations satisfied the properties, empirical interpretations are necessary. In the following paragraphs, we thus discuss choices made with respect to evaluation.

When calculating the faithfulness correlation, it is important to be aware of the risk that perturbing the input can create out-of-distribution samples as well as spurious correlations of the input features. Therefore, we choose the following three different pixel perturbation methods: replacement by black pixels, by the mean of the neighboring pixels as well as by a random float value between the minimum and maximum value of the neighboring pixels. Furthermore, we conduct the experiments with three different sizes of the pixel-patches $\{1, 2, 4\}$ that are perturbed at each step. The faithfulness values in the experimental results are reported as average values with a standard deviation of the combination of all settings, i.e., baseline choices and patch sizes. In this way, we hope to portray a more reliable picture of what explanation-enhancing method is most faithful to the model, independent of the choice of baseline and patch size.

For the localization criteria, we reported AUC and $dAUC$. The "*delta AUC*" is computed in order to clearly see the relative increase (or decrease) that different settings of NG++ results in and is defined as follows: $(AUC_{NG++} / AUC_{Baseline}) - 1$. Lastly, for the robustness metric, we added Gaussian Noise to the perturbed input $\delta \sim \mathcal{N}(0, \sigma^2)$ such that $\sigma^2 = 0.05$.

D.2 Datasets and pre-processing

In our experiments, we use two datasets where pixel-wise placements of the explainable evidence of the attributions were made available.

CMNIST. For constructing the semi-natural dataset, we combined two well known datasets; the MNIST dataset [23], consisting of 60,000 train- and 10,000 test grey-scale images and the CIFAR-10 dataset, consisting of 50,000 train- and 10,000 test colored images. Each MNIST digit (0 to 9) was first resized from (28, 28) to (16, 16) and then rotated randomly, with a maximal rotation degree of 15. Afterwards, those digits were added on top of CIFAR images of size (32, 32), which were uniformly sampled, such that there exists no correlation between CIFAR and MNIST classes. Hence, within this experimental setup, we could assume that the model does not rely on the background for the decision-making process. Using this constructed semi-natural dataset in the experiments, random noise of varying variance σ^2 was added to each CMNIST image.

As a pre-processing step, all images were normalized. For the training set, the random affine transformation was also applied to keep the image center invariant. The random rotation ranges withing $[-15, 15]$ degrees, random translations, scaling and shearing in the range of $[0.95, 1]$ and $[0, 0.05]$ percents respectively using the fill color 0 for standard `torchvision.transforms.RandomAffine` data augmentation in PyTorch [56]. We constructed three different ground-truth segmentation masks for the CMNIST dataset as follows: squared box around the digit, the digit segmentation itself and the digit plus neighborhood of 3 pixels in each direction. In the experiments, as the evidence for a class typically also is distributed around the object itself, the squared box of (16, 16) pixels was selected as the single ground-truth segmentation.

PASCAL VOC 2012. We use PASCAL Visual Object Classes Challenge 2012 (VOC2012) [57] to evaluate our method on a natural high-dimensional segmented dataset. For training and evaluation, we resize images such that the number of pixels on one axis is 224 pixels and perform center crop afterward, resulting in square images of 224×224 pixels. Images are then normalized with standard ImageNet mean and standard deviation. The segmentations are also resized and cropped, accordingly. For the training we augment the data with random affine transformations that include random rotation in the range $[-30, 30]$ degrees, random translations, scaling and shearing in the range of $[0, 5]$. Additionally, we perform horizontal and vertical random flips with a probability of 0.5.

D.3 Explanation methods

In this section, we provide a brief overview of the explanations methods used in the experiments conducted in both the main manuscript and the supplementary material. For each explanation method, we use absolute values of the attribution maps, following the same logic as in [8]. This is motivated by the fact that both positive and negative attributions drive the final prediction score.

Saliency. Saliency (SA) [43] is used as the baseline explanation method. The final relevance map quantifies the possible effects of small changes in the input on the output produced

$$E_{Saliency}(\mathbf{x}, f(\cdot, W)) = \frac{\partial f(\mathbf{x}, W)}{\partial \mathbf{x}}.$$

Integrated Gradients. Integrated Gradients (IG) [6] is an axiomatic local explanation algorithm that also addresses the "gradient saturation" problem. A relevance score is assigned to each feature by approximating the integral of the gradients of the models' output with respect to a scaled version of the input [6]. The relevance attribution function for IG is defined as follows

$$E_{IG}(\mathbf{x}, f(\cdot, W)) = (\mathbf{x} - \bar{\mathbf{x}}) \int_0^1 \frac{\partial f(\mathbf{x} + \alpha(\mathbf{x} - \bar{\mathbf{x}}), W)}{\partial \mathbf{x}} d\alpha,$$

where $\bar{\mathbf{x}}$ is a *reference point*, which is chosen in a way that it represents the absence of a feature in the input.

LRP. Layer-wise Relevance Propagation [2] is a model-aware explanation technique that can be applied to feed-forward neural networks and can be used for different types of inputs, such as images,

videos, or text [58, 59]. Intuitively, the core idea of the LRP algorithm lies in the redistribution of a prediction score of a certain class towards the input features, proportionally to the contribution of each input feature. More precisely, this is done by using the weights in combination with the neural activations that were generated within the forward pass as a measure of the relevance distribution from the previous layer to the next layer until the input layer is reached. Note that this propagation procedure is subject to a conservation rule – analogous to Kirchoff’s conservation laws in electrical circuits [60] – meaning, that in each step of back-propagation of the relevances from the output layer towards the input layer, the sum of relevances stays the same.

In the experiments we deploy LRP gamma rule i.e., LRP- γ which dependent on the tuning of γ can favor the positive attributions over negative ones. As we increase γ , negative contributions start to cancel out. The LRP gamma rule is defined as follows

$$R_j = \sum_k \frac{a_j \cdot (w_{jk} + \gamma w_{jk}^+)}{\sum_{0,j} a_j \cdot (w_{jk} + \gamma w_{jk}^+)} R_k \quad (8)$$

where γ controls how much positive contributions are favoured, j and k are neurons at two consecutive layers of the network, a_j are attributions, w are weights and R_k are relevances.

GradShap. Gradient Shap [20] is a local explainability method that approximates Shapley values of the input features by computing the expected values of the gradients when adding Gaussian noise to each input. Since it computes the expectations of gradients using different reference points, it can be viewed as an approximation of IG.

D.4 Additional results

In Table 3 and Table 4, we present AUC scores for all the model architectures that were trained for CMNIST, using the recommended heuristic to set the noise level. For these calculations, we also updated the value for σ_{SG} (see Eq.5) following the authors’ recommendation of the interval from 0.1 to 0.2. In the main manuscript’s Table 2, we reported results that were computed using a slightly lower σ_{SG} of 0.05. That being said, the results in both the main manuscript and the supplementary material are coherent, where NG and NG++ using the recommended heuristic significantly perform best.

Table 3: Resulting AUC scores for different architectures

Method	LeNet	VGG11	ResNet9	ResNet18	ResNet50
Base	0.922 ± 0.033	0.961 ± 0.017	0.926 ± 0.026	0.913 ± 0.04	0.912 ± 0.035
SG	0.940 ± 0.048	0.971 ± 0.025	0.975 ± 0.015	0.962 ± 0.026	0.967 ± 0.022
NG	0.949 ± 0.029	0.982 ± 0.011	0.978 ± 0.012	0.963 ± 0.023	0.973 ± 0.017
NG++	0.961 ± 0.025	0.984 ± 0.011	0.982 ± 0.011	0.975 ± 0.016	0.969 ± 0.019

Table 4: Resulting AUC scores for different architectures

Method	VGG16	ResNet34	ResNet101
Base	0.967 ± 0.015	0.925 ± 0.028	0.934 ± 0.027
SG	0.963 ± 0.034	0.968 ± 0.023	0.973 ± 0.018
NG	0.985 ± 0.011	0.979 ± 0.012	0.978 ± 0.011
NG++	0.982 ± 0.013	0.981 ± 0.011	0.980 ± 0.012

D.5 Models and training results

Each model was trained in a similar manner; using a standard cross entropy loss (`torch.nn.CrossEntropyLoss` in PyTorch) – the LeNet and ResNet networks were trained using the AdamW variant [61], with an initial learning rate of 0.001 and the VGGs were trained using stochastic gradient descent with an initial learning rate of 0.01 and momentum of 0.9. The training

was completed for 20 epochs for all models. Furthermore, ReLU activations were used for all layers of the networks apart from the last layer, which employed a linear transformation. For details on model architectures we point the reader to the original source; LeNet [46], ResNets [44] and VGG [45] respectively.

In Table 5, the reader can find the model performance listed (both training- and test accuracies). For the sake of space, we refer to each ResNet as RN.

Table 5: Training results for different architectures

Acc.	LeNet	VGG11	VGG16	RN9	RN18	RN34	RN50	RN101
Train	0.7841	0.9237	0.9508	0.9723	0.9747	0.9734	0.9754	0.9760
Test	0.8653	0.9634	0.9797	0.9850	0.9864	0.9868	0.9898	0.9885

In the PASCAL VOC 2012 dataset, we trained a ResNet18 for multi-label classification, changing the number of output neurons to 20 to represent the number of classes in dataset. The network was trained with Binary Cross-Entropy loss applied on top of sigmoid layer (`torch.nn.BCEWithLogitsLoss` in PyTorch). ResNet 18 was initialized with ImageNet [62] pre-trained weights (available in `Torchvision.models`) and was trained for 100 epochs with SGD with 0.01 learning rate and with 100 epochs with a learning rate of 0.005. The network achieves a loss of 0.000295 on the training dataset and 0.000376 on the test dataset.

For the illustrations in this Appendix, we used a VGG 16 [45] model pretrained on ImageNet (available in `Torchvision.models`).

E Broader Impact

Although the use of machine learning algorithms in various application areas, such as autonomous driving or cancer cell detection, has produced astonishing achievements, the risk remains that these algorithms will make incorrect predictions. This poses a threat, especially in safety-critical areas as well as raises legal, social and ethical questions. However, in times of advancing digitization, the deployment of artificial intelligence (AI) is often decisive for competitiveness. Therefore, methods for a thorough understanding of the often highly complex AI models are indispensable. This is where the field of explainable AI (XAI) has established itself and in recent years various XAI methods for explaining the "black-box models" have been proposed. In general, more precise and reliable explanations of AI models would have a crucial contribution to ethical, legal and economic requirements, the decision-making basis of the developer and the acceptance by the end-user.

In particular, it has been shown with the explanation-enhancing SmoothGrad method, that small uncertainties, which are artificially added to the input space can lead to an improvement in the explanation. In this work, we propose a novel method, where the uncertainties are not introduced to the input space, but to the parameter space of the model. We were able to show in various experiments that this leads to a significant improvement when it comes to attribution quality of explanations, measured with different metrics and subsequently can be beneficial in practice. In case the proposed method does not provide a localized, robust and faithful explanation, this would have no direct consequences for the user as long as the explanation is used for decision support and is not a separate decision unit. The data we use does not contain any personal data or any offensive content.

F Illustrations

We provide further explanations of SmoothGrad, NoiseGrad and NG++ for several ImageNet images [62]. Here, we used a VGG-16 network pretrained on ImageNet and the explanations of Saliency, Integrated Gradients, Gradient SHAP and LRP- γ are shown in Figure 9-11.

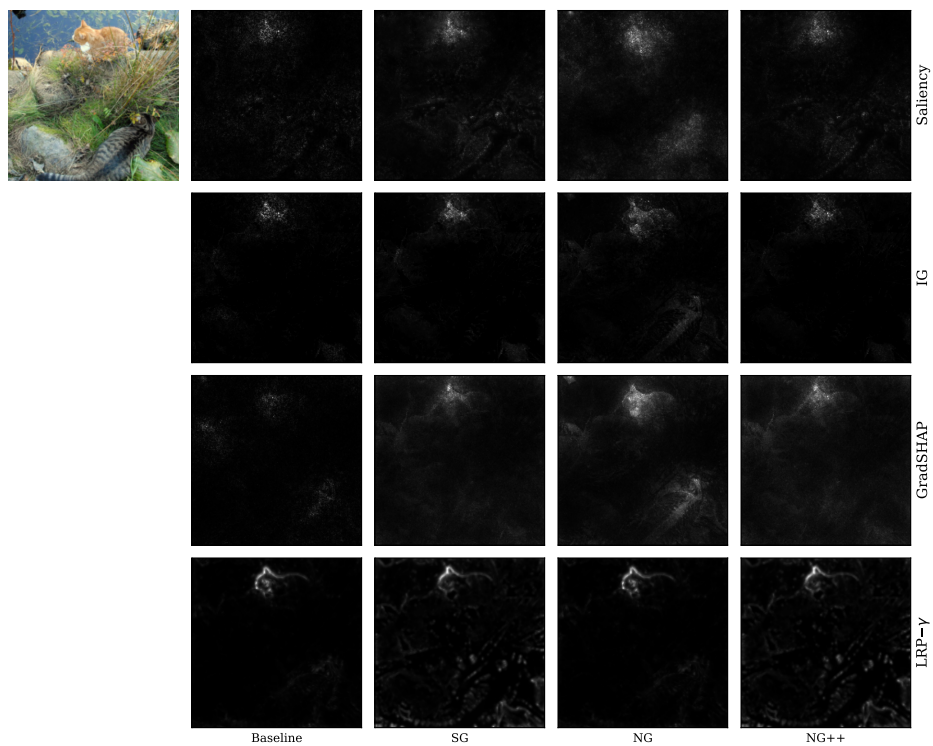


Figure 9: Comparison of different enhancing methods for class "tiger cat".

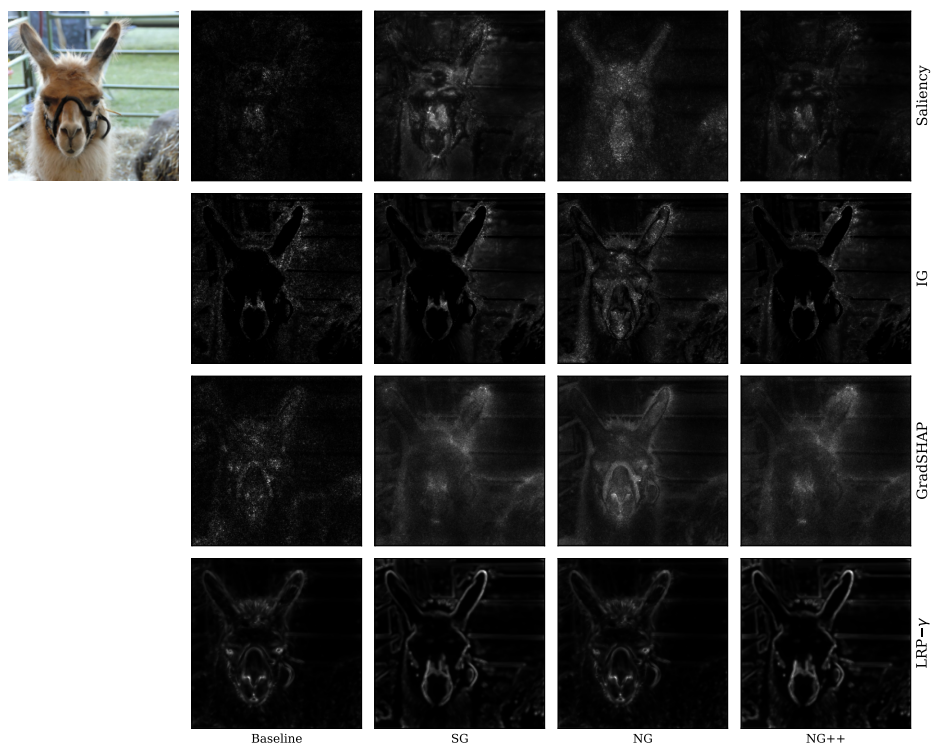


Figure 10: Comparison of different enhancing methods for class "lama".

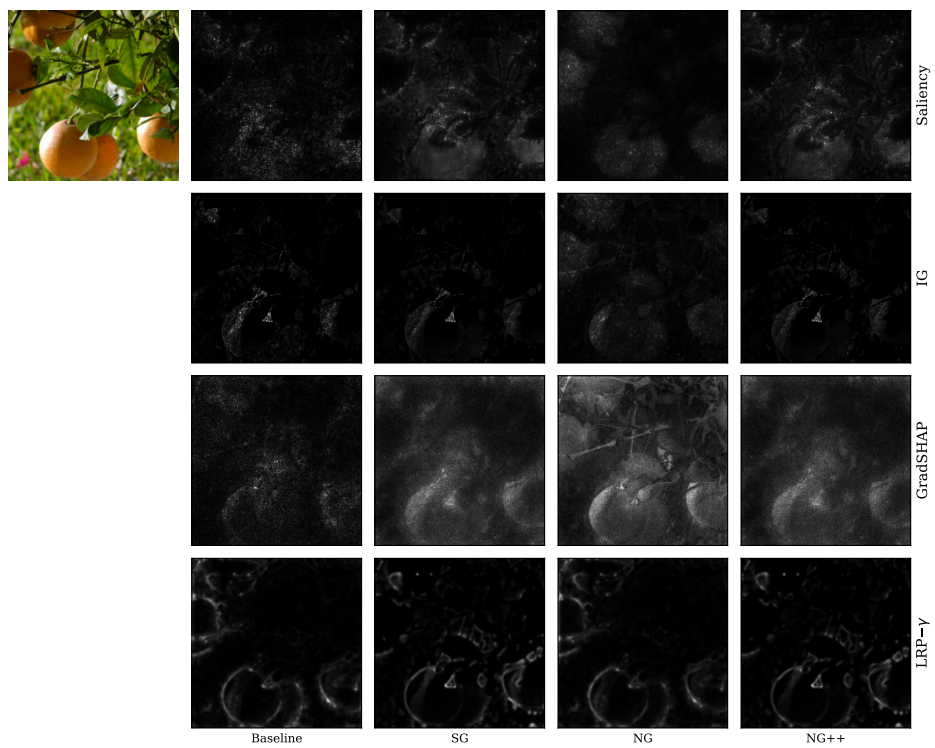


Figure 11: Comparison of different enhancing methods for class "lemon".